17 (2023) 100280

Contents lists available at ScienceDirect

International Journal of Thermofluids

journal homepage: www.sciencedirect.com/journal/international-journal-of-thermofluids

Dynamic modelling and analysis of Organic Rankine Cycle power units for the recovery of waste heat from 110kW Proton Exchange Membrane Fuel cell system

Tabbi Wilberforce *, Imran Muhammad

Department of Mechanical Engineering and Design, Aston University, United Kingdom

ARTICLE INFO

Keywords:
Mass flowrate
Organic rankin cycle
Proton exchange membrane fuel cell
Working fluid

ABSTRACT

The recovery of waste heat from Proton Exchange Membrane (PEM) Fuel cell is sin qua non to the development of organic Rankin cycle units. Despite the appreciable increase in the sale of PEM fuel cell units in 2021, the waste heat from some of these fuel cell units is typified by large fluctuations in mass flow rate as well as temperature which is more likely to affect the overall performance of an organic Rankine cycle (ORC) unit when coupled to a fuel cell. It is therefore imperative that the dynamic modelling of the Proton Exchange Membrane Fuel cell and organic Rankine cycle integrated system is developed to analyse the performance of the integrated system. This also involves the development of an appropriate control strategy for guaranteeing safer and optimum performance of the integrated system. The developed Proportional, Integral, Derivative (PID) control unit is able to maintain the thermal efficiency of the ORC system at 10% subject to the mass flow rate of the waste heat as well as the working fluid and also ensure safe operation of the integrated system. There is a 0.9% increase in the output power of the PEMFC after 2000 seconds of operation clearly highlighting the contribution of the integrated system in improving the overall output power being harnessed.

1 Introduction

As the world continue to strive for environmentally friendly medium of harnessing energy [1], renewable energy is however projected as suitable replacement for fossil-based commodities [2–4]. Proton exchange membrane fuel cells (PEMFC) remains promising due to their higher performance. PEMFC's are environmentally friendly and exhibit a fast start up time unlike other energy converting devices [5]. Due to its peculiar benefits for vehicle applications, such as high energy conversion efficiency, low start-up temperature, and no moving components, the proton exchange membrane fuel cell (PEMFC) has become one of the most attractive alternative power sources [6]. Many parameters, including operational temperature, pressure, and reactant concentration, restrict the maximum output voltage of a single cell PEMFC [7]. In order to meet the requirement for automotive applications, PEMFCs must be connected in series to create a fuel cell stack.

The reactant concentration as well as pressure in various cells of a fuel cell stack usually vary, resulting in differences in cell temperature, reactant humidity, or water distribution. Furthermore, practical cell operating conditions such as frequent thermal cycling, humidity cycling, wet-dry cycling, and vibrations can significantly degrade cell performance coupled with durability [8,9]. As a result, an effective energy management system for PEMFC is becoming more important. The performance of a PEMFC system is highly dependent on its design and operational conditions. Due to its speed, efficiency, and cost, numerical modelling has been used by many researchers to study various design and operating factors. Baschuk and Li [10] developed a mathematical model of a PEMFC stack that uses hydraulic network analysis to predict the pressure and mass flow rate distributions for the reaction gases.

They discovered that homogeneous reactant redistribution is crucial to stack efficiency, and strategies to improve mass flow homogeneity were developed. The reactant and coolant channel design [11], pressure [12], temperature [13], and even co-poisoning [14] impacts are all examined using comparable fuel cell stack modelling methodologies. The PEMFC system for automobiles additionally comprises of a hydrogen system, an air system, and various ancillary systems in addition to the stack. On the anodic electrode, the hydrogen pressure can be adjusted to vary the flow conditions at the high-pressure hydrogen tank's exit, as well as the extra hydrogen after the fuel cell stack can be recycled using mechanical pumps, compressors, and even ejectors [15,16]. On the oxygen side, an air compressor is required to compress the

* Corresponding author.
E-mail address: t.awotwe@aston.ac.uk (T. Wilberforce).

https://doi.org/10.1016/j.ijft.2023.100280

Available online 8 January 2023

Nomenclature

Parameters

A	Area (m^2)
A_o	cross-sectional area of valve (m^2)
C_P	Heat capacity at constant pressure ($J\ K^{-1}$)
C_d	Discharge coefficient (-)
CS(t)	Control signal (-)
CV	Control variable (-)
h	Specific enthalpy ($J\ kg^{-1}$)
K_{eq}	Stodola's constant (-)
$\dot{m}$	Mass flow rate ($kg\ s^{-1}$)
n	No. of control volumes (-)
ORC	Organic Rankine Cycle (-)
p	Pressure (bar)
PI	Proportional integral (-)
PID	Proportional integral derivative (-)
PV	Process variable (-)
$\dot{Q}$	Heat flow rate (W)
SP	Set point (-)
T	Temperature (K)
t	Time (sec)
U	Internal energy (J)
V	Volume (m^3)
v	Specific volume ($m^3\ kg^{-1}$)
$\dot{W}$	Power (W)
X	Pump capacity faction (-)

Greek symbols

ρ	Specific density ($kg\ m^{-3}$)
η	Efficiency (%)
ϕ	compressibility coefficient (-)
γ	Heat capacity ratio (-)

Subscripts and superscripts

hs	Heat source
w	Wall
wf	Working fluid
pp	Pump
exp	expander
i	In
o	out
cv	Valve

air to provide correct flow and pressure into the stack, and good matching of the PEMFC stack and air compressor may increase overall system efficiency [12]. Humidification is also important for PEMFC efficiency, and alternative techniques can be used to obtain the right humidification threshold of reactant gases, with the membrane humidification method being the most preferable option for vehicular applications due to its simple structure as well as fairly decent efficiency.

Through correct design and matching of the aforesaid sub-systems, system efficiency may be further increased by lowering energy usage. A group of researchers used empirical and semi-empirical models based on artificial neural networks and semi-empirical equations to probe into the operational improvement of a PEMFC system, and they discovered that the efficiency gaps between the worst and best operation conditions of the system could reach 1.2–5.5 percent [17]. The research and application progress of PEMFC waste heat recovery is far behind the research and application progress of key components and system control owing to its poor grade. Some academics have been interested in PEMFC waste heat recovery in recent years, and have proposed some waste heat recovery solutions [18,19]. However, similar studies [20] are only restricted to theoretical concepts, and their practical application is limited due to the overly complicated system structure. As a result, testing a simple and efficient waste heat recovery strategy for low-temperature PEMFC is critical. The organic Rankine cycle (ORC), which is a closed energy harvesting power cycle that uses an organic fluid with a low boiling point [21], has been widely investigated as a promising energy harvesting technique for recovering thermal energy from low-grade thermal sources such as geothermal sources [22], solar energy, and internal combustion engine exhaust gases. Due to its low evaporation and condensation temperatures, high power production efficiency, simple equipment, and environmentally benign operation, the ORC approach is ideal for thermal energy harvesting [23]. Hung et al. [24] explored several organic fluids for ORC systems below 80°C, and their findings showed that wet fluids with extremely steep-saturated vapour curves in the T-s diagram outperformed dry fluids. Wang et al. [25] used a thermodynamic model to analyse the physical and chemical characteristics of nine different kinds of organic working fluids in order to determine the impact of their physical and chemical qualities on the ORC system efficiency for engine waste heat recovery. Their findings imply that R11, R141b, R113, and R123 are more efficient than others, whereas R245fa and R245ca are more environmentally friendly. Ebrahimi and Moradpoor [26] studied the influence of 10 design factors on the cycle performance, which included solid oxide fuel cells, micro-gas turbines, and organic Rankine cycles. The integrated system is shown to cut fuel consumption by 45 percent and achieve over 65 percent energy conversion efficiency under ideal design parameters. Meanwhile, they said it would be better if it was combined with modern thermally actuated cooling systems. To collect thermal energy from an internal combustion engine, Shu et al. [27] integrated the thermoelectric generator (TEG) and ORC based on R123 as the working liquid. The combined TEG-ORC system seems to enhance the effectiveness of collecting waste heat from engines, according to the findings. Wang et al. [28] presented a low-temperature solar Rankine system using R245fa as the circulatory system's working fluid. According to the findings, depending on the operating circumstances, conversion efficiency may reach 4.2 percent or 3.2 percent. Chang et al. [29] investigated a solar-energy and high-temperature PEMFC-based CCHP system, as well as a high-temperature PEMFC-based CCHP system that didn't use solar energy. With the addition of solar energy, the pollutant emission reduction rates (ERRs) of the system may be raised by roughly 8.4 percent -23.5 percent, according to the findings. Chang et al. [30] looked into a hybrid PEMFC-solar energy CCPH system based on the ORC cycle and vapour compression cycle and discovered that the system's average efficiency is 75.4 percent in the summer and 85.0 percent in the winter. The energy harvesting based on ORC has been researched for many

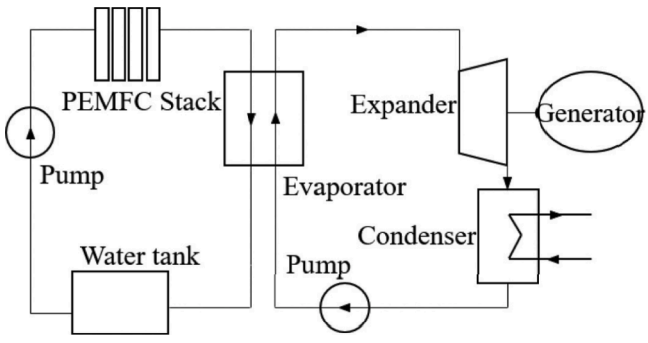

Fig. 1. Diagram for the proton exchange membrane fuel cell and the organic Rankine cycle unit.

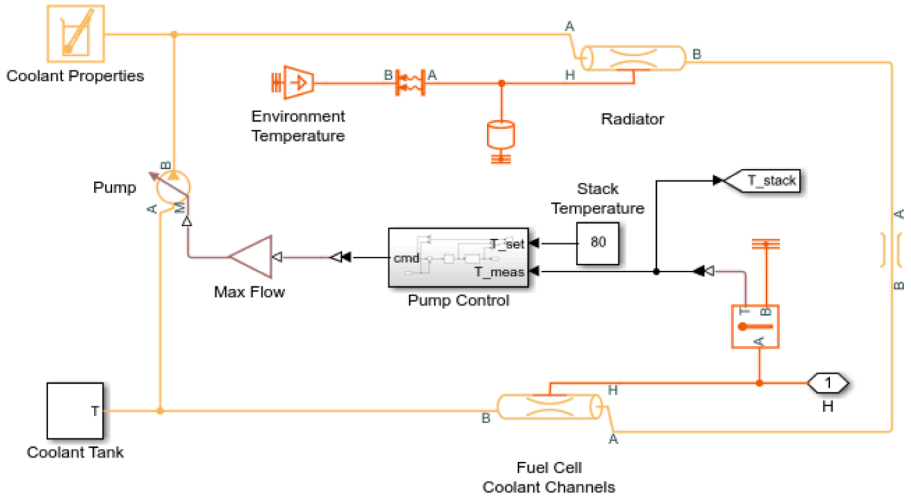

Fig. 2. Cooling system for the PEM fuel cell unit.

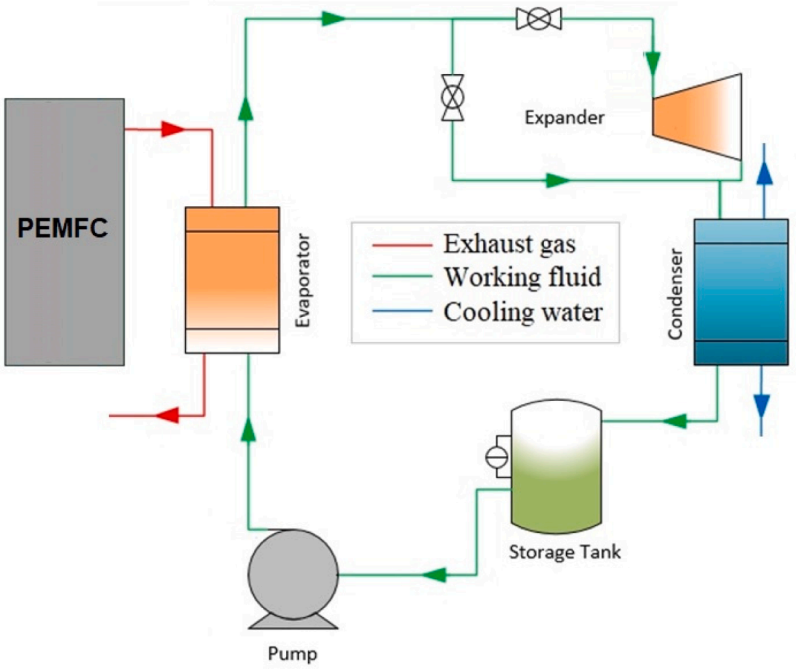

Fig. 3. Diagram for the ORC units used in the investigation.

thermal sources, as can be observed from the above study. However, its viability and advantages for low-temperature PEMFC energy recovery have yet to be examined in detail. As a result, the goal of this research is to create a theoretical model that uses the ORC system to collect low-grade heat energy from a PEMFC cooling system, as well as to thoroughly analyse the elements that impact the combined system's efficiency. For the existing PEMFC-ORC system, a comparison of several kinds of working fluid (R134a and R245fa) is undertaken. To attain optimal performance, a parametric analysis is conducted for the integrated system. This PEMFC-ORC system and associated research discoveries have increased relevance for future practical use due to its simplicity and practicability. Section 2 of the study presents the methodology adopted in the present study with some specific assumptions discussed. This is then followed by Section 3 where the developed ORC model is presented and explained. Section 4 captures the control unit for the ORC system whiles the result and discussion for the study is presented in Section 5. Section 6 presents a brief summary of outcome of the study with some future research directions enumerated.

2. Formulation of approach

To improve the efficiency of a proton exchange membrane fuel cell, an organic Rankine cycle unit is attached to recoup dissipated heat via the cooling water in a fuel cell cooling system. An evaporator is utilised as replacement for a fuel cell cooling unit as highlighted in Fig. 1. The primary source of heat for the organic Rankine cycle unit originates from the high temperature cooling water instead of the heat being dissipated

Table 1
Design point for the ORC unit for the recovery of waste heat from PEMFC.

Heat source		Working fluid			
Mass flow rate (kg/s)	Temperature (K)	Evaporation temperature (K)	Condensation temperature (K)	Degree of superheat (K)	Mass flow rate (kg/s)
0.348	80	75	313	2.5	0.142

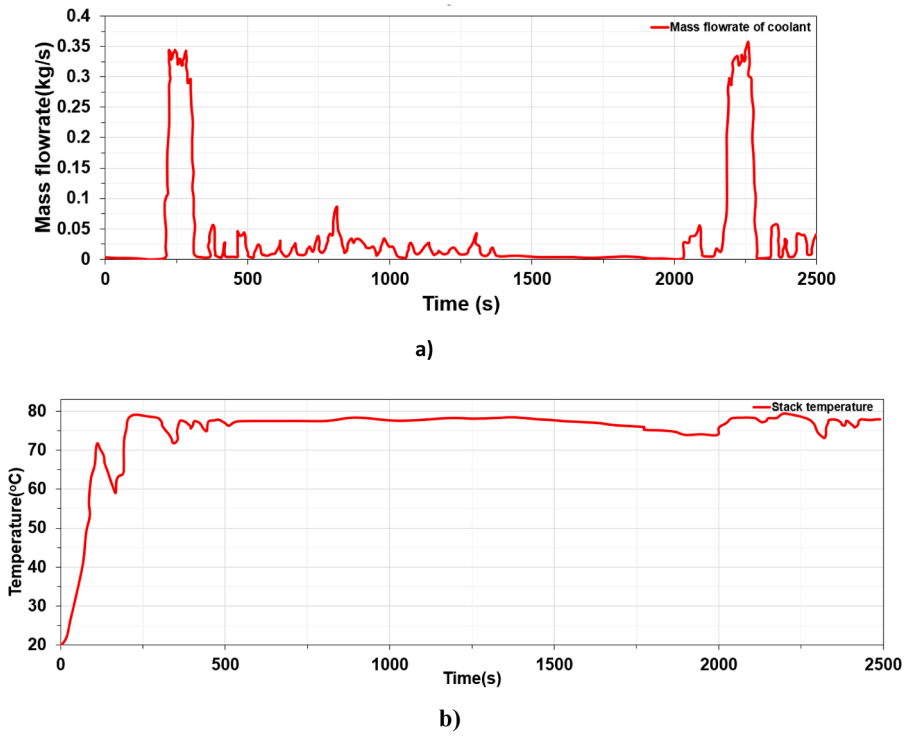

Fig. 4. : a) Mass flow rate of waste heat b) Temperature of the heat from the cooling system for the fuel cell unit.

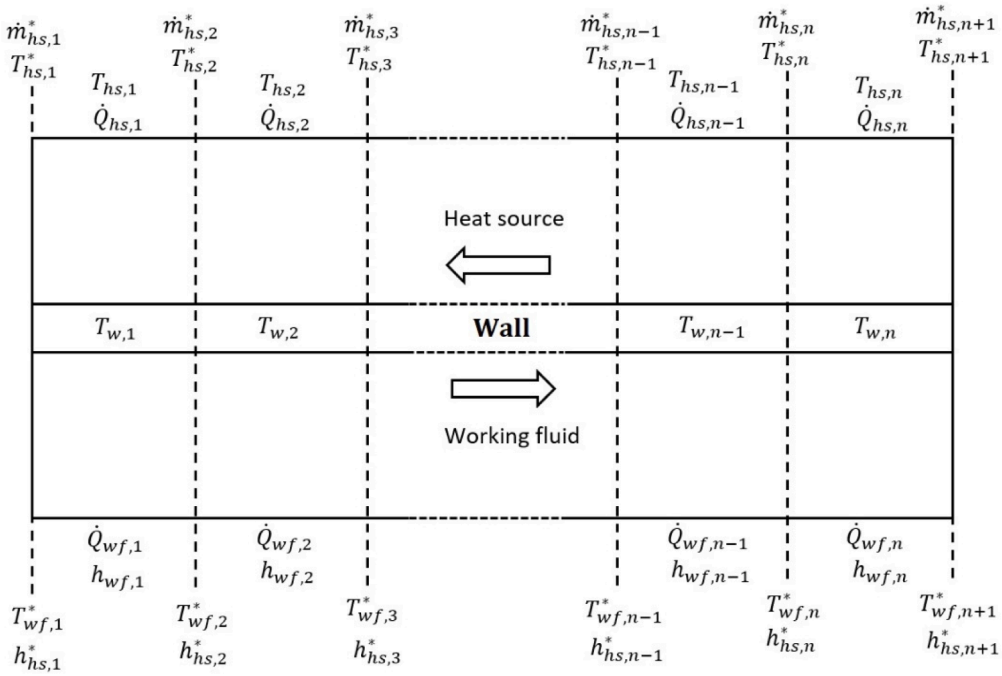

Fig. 5. One dimensional model for the heat exchanger [33].

into the atmosphere. Heat is absorbed from the working fluid at high pressure within the evaporator. This is then transformed from a liquid state to a saturated vapour state. The high pressure coupled with the high temperature vapor is then utilised in driving the high efficiency turbine leading to the production of electricity. The combined PEMFC-ORC unit is developed in this study based on a single fuel cell model; stack model coupled with an organic Rankine cycle model.

To make the system analysis simplified, the following assumptions are factored into the study. Firstly, all of the system's components are in a constant state, and heat and pressure losses are negligible. Secondly, the temperature outside is 20°C, and the pressure is 101 kPa. Furthermore, the chemical process reaches a point of equilibrium. Again, the fuel cell gas flow pathways have constant and equal pressures. Moreover, the gas temperature at the PEMFC stack's output is constant and

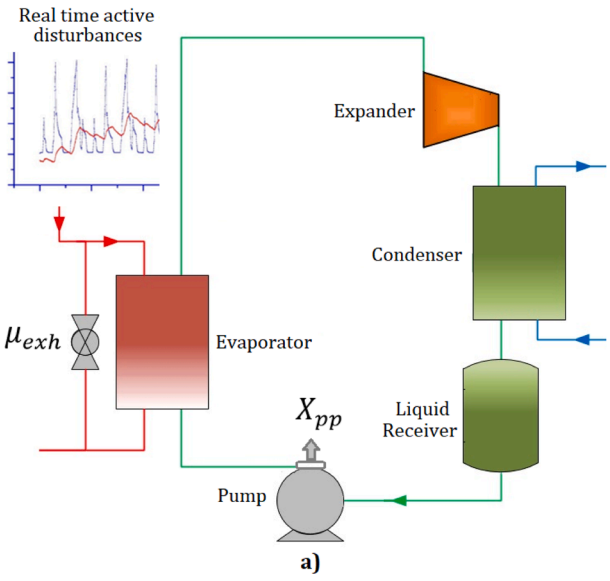

Fig. 6. Controller configuration of the organic Rankine system [36].

equal to the stack's operating temperature. To examine the influence of running current, temperature, and pressure on cycle/system efficiency, the aforementioned model may be created and executed in Simulink. The model's perculia explanation is provided in the following subsections.

2.1. Single proton exchange membrane fuel cell model

For a single cell proton exchange membrane fuel cells, the voltage at the output is determined based on the losses within the cell and this is deduced from Eq. (1) [31].

$$E_{cell} = E_{rev} - V_a - V_o - V_c \tag{1}$$

The output voltage is denoted as E_{cell} whiles the activation losses is represented as V_a. Losses due to the material composition of the membrane which is often referred to as the ohmic losses is represented as V_o and that of the concentration losses is V_c. Eq. (2) which is the next voltage is another method that can be utilised in the determination of the reversible voltage [31].

$$E_{rev} = \frac{\Delta G}{2F} + \frac{\Delta S}{2F}(T - T_{ref}) + \frac{RT}{2F}\ln\left[\left(\frac{C_{H_2}}{C_{H_2}^{ref}}\right)\left(\frac{C_{O_2}}{C_{O_2}^{ref}}\right)^{\frac{1}{2}}\right] \tag{2}$$

The Gibbs free energy is ΔG whiles the Fraday's constant is captured as F. The entropy is ΔS and the cell operating temperate is T. The reference temperature is T_{ref} whiles the universal constant is R. The fuel concentration is denoted as C_{H_2} whiles that of the reductant is C_{O_2}. The concentration for both the reductant and fuel at the reactive site is captured as $C_{O_2}^{ref}$ and $C_{H_2}^{ref}$ respectively from Eq. (2).

Electrochemical kinetics and electron and proton adsorption in both the anode and cathode catalyst layers create the activation overpotential V_a [32]. The circuit resistance owing to proton and electron migration causes the ohmic overpotential V_o. The mass transport restrictions cause the concentration overpotential V_c. V_a, V_o, and V_c values alter as the stack load varies [32].

3. Organic Rankine Cycle model

The heat dissipated from the fuel cell which would have been wasted is obtained via a cooling system as shown in Fig. 2. A diagram for the approach adopted in the recovery of waste heat via ORC is presented in Fig. 3. Table 1 highlights specific design points with the working fluid being R245fa for the organic Rankine system.

The heat source data were obtained from the cooling system during the operation of the fuel cell. Fig. 4 captures the variation for the mass flow rate as well as the temperature from the cooling system.

3.1. Dynamic model

Development of the dynamic model was executed in a Modelica language. This language is also described as an object-oriented modelling language. The model is made up of systems obtained from the Thermocycle library [33]. Validation of the individual components coupled with the organic Rankine cycle unit have already been executed from the transient and steady state investigation conducted by Desideri et al [34] using 11 kW organic Rankine cycle unit. The net output power was re-generated with an accuracy of 5 percent whiles that of the expander inlet pressure was recorded as 10 percent. Computations for the working fluid was determined with the aid of an external media library [35].

3.2. Model for the heat exchanger

The boundary layer coupled with the finite volume approach are the two often used approach for the dynamic modelling for the heat exchanger. The current investigation adopts the finite volume method for modelling the heat exchanger. Flow length for the heat exchanger is subclassified into 'n' even control volumes. Once that is carried out, for each of the control volume, law of conservation of energy and mass is then applied. Fig. 5 captures the discretized 1-dimensional model for the

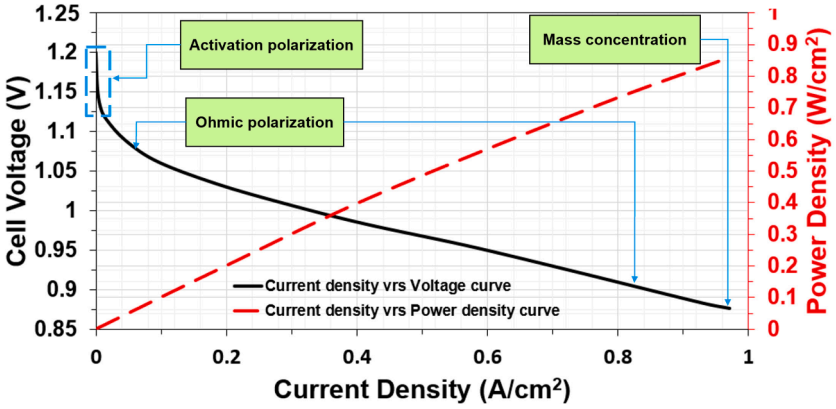

Fig. 7. Overall performance of the proton exchange membrane fuel cells under investigation.

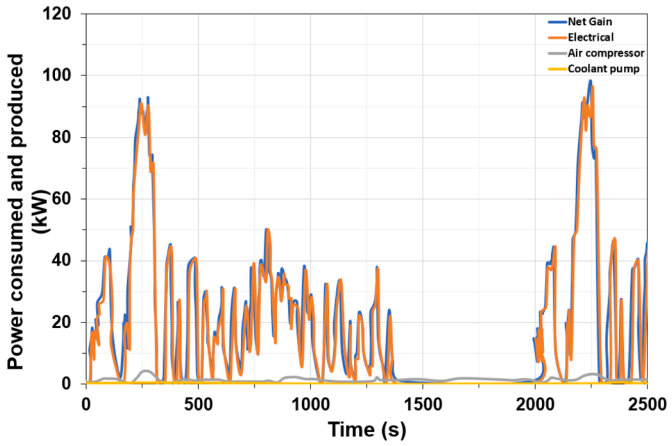

Fig. 8. The total power generated by the fuel cell and that consumed.

heat exchanger.

Momentum balance was assumed to be negligible. Similarly, variation of the fluid characteristics was noted to only occur in the direction of the flow. The characteristics for the fluid was computed for the individual volume at the mean states for the 2 nodes denoted as "*" from Fig. 5. Taking the individual cells into account, area, mass as well as volume for the fluid is denoted by;

$$A_i = \frac{A}{n};\ V_i = \frac{V}{n};\ A_i = \frac{\dot{m}}{n}; i = 1, 2, 3\cdots\cdots n \tag{3}$$

For the individual side for the heat exchanger the mass balance is calculated from Eq. (4).

$$A\frac{\partial \rho}{\partial t} + \frac{\partial \dot{m}}{\partial x} = 0 \tag{4}$$

$$\frac{d\dot{m}_i}{dt} = V_i\left[\frac{\partial \rho}{\partial h}\frac{dh}{dt} + \frac{\partial \rho}{\partial p}\frac{dp}{dt}\right] = \dot{m}_i^* - \dot{m}_{i-1}^*$$

The energy balance is also calculated using Eq. (5).

$$\frac{dU_i}{dt} = \left(\dot{m}_{i-1}^* h_{i-1}^* - \dot{m}_i^* h_i^*\right) + \dot{Q}_i - p\frac{dV_i}{dt} \tag{5}$$

$$V_i\rho_i\frac{\partial h_i}{\partial t} = \dot{m}_{i-1}^*\left(h_{i-1}^* - h_{i-1}\right) - \dot{m}_i^*\left(h_i^* - h_i\right) + \dot{Q}_i - p\frac{dV_i}{dt}$$

3.3. Model for the expander and pump

Due to the dynamics for the pump coupled with the turbine being fast as well as their time constant being lower compared to heat exchangers, lumped model centred around empirical correlations without taking into account the dynamics is utilised for the pump as well as turbine. Semi – empirical formulation using Stodola equation is utilised in computing the mass flow rate for the working fluid via the turbine indicated below.

$$\dot{m}_{wf,exp} = K_{eq}\sqrt{\rho_{i,exp}p_{i,exp}\left(1 - \left(\frac{p_{i,exp}}{p_{o,exp}}\right)^{-2}\right)} \tag{6}$$

$$K_{eq} = \frac{\dot{m}_{wf,exp}}{\sqrt{2\rho_{i,exp}\left(p_{i,exp} - p_{o,exp}\right)}} \tag{7}$$

85 percent was however assumed as the isentropic efficiency for the turbine whiles the outlet enthalpy for the turbine was also deduced using eqn. 8.

$$h_{o,exp} = h_{i,exp} - \eta_{exp,is}\left(h_{in,exp} - h_{is,exp}\right) \tag{8}$$

Using a third order polynomial also defined as capacity fraction from a pump flow fraction, X_{pp}, the pump's isentropic efficiency was deduced using Eqn. 9.

$$\eta_{is,pp} = a_0 + a_1\log\left(X_{pp}\right) + a_2\log\left(X_{pp}\right)^2 + a_3\log\left(X_{pp}\right)^3 \tag{9}$$

The capacity fraction for the pump is defined using eqn. 10.

$$X_{pp} = \frac{v_{i,pu}\dot{m}_{wf,pp}}{V_{in,pp,max}} \tag{10}$$

Power consumption coupled with the outlet temperature for the pump is equally denoted by eqn. 11 and 12.

$$\dot{W}_{pp} = \frac{\dot{m}_{wf}}{\rho}\frac{\left(p_{o,pp} - p_{i,pp}\right)}{\eta_{is,pp}} \tag{11}$$

$$T_{o,pp} = T_{i,pu} + \frac{\left(1 - \eta_{is,pp}\right)}{\dot{m}_{wf,pp} \times C_{p,pp}}P_{pp} \tag{12}$$

3.4. Model for the liquid receiver

At all times, the liquid and vapour phases in the storage tank are considered to be in thermodynamic equilibrium, i.e., the vapour as well as liquid are expected to be saturated at specified pressure. Mass balance is calculated from Eqn. 13:

$$\frac{d\dot{m}_{wf}}{dt} = \dot{m}_{i,wf} - \dot{m}_{o,wf};\ \frac{d\dot{m}_{wf}}{dt} = V.\left[\frac{\partial \rho}{\partial h}.\frac{dh}{dt} + \frac{\partial \rho}{\partial p}.\frac{dp}{dt}\right] \tag{13}$$

3.5. Valve model

Determination of the drop in pressure across the valve is determined based on quadratic expression with the aid of incompressible flow hypothesis. In the case of incompressible flow, mass flow rate is determined using Eq. (14).

$$\dot{m}_{wf,cv} = \mu_{cv}C_dA_O\sqrt{\rho_{in}p_{in}\phi} \tag{14}$$

The compressibility coefficient is ϕ is also calculated using eqn. 15.

$$\phi = \frac{2\gamma}{\gamma - 1}\left(\psi^{\frac{2}{\gamma}} - \psi^{\frac{\gamma+1}{\gamma}}\right),\ \text{where}\ \gamma = \frac{C_p}{C_v} \tag{15}$$

The factor, ψ, depends on the flow condition and is computed from eqn. 16.

$$\psi = \begin{cases} \frac{p_o}{p_i}\ if\ \frac{p_o}{p_i} > \left(\frac{2}{\gamma+1}\right)^{\frac{\gamma}{\gamma-1}}\ subsonic \\ \left(\frac{2}{\gamma+1}\right)^{\frac{\gamma}{\gamma-1}}\ if\ \frac{p_o}{p_i} \le \left(\frac{2}{\gamma+1}\right)^{\frac{\gamma}{\gamma-1}}\ supersonic \end{cases} \tag{16}$$

K_{eq}comprises of equivalent inlet nozzle cross section as well as discharge coefficient often referred to as Stodolaś constant.

Eqn. 7 presents a mathematical expression for K_{eq}

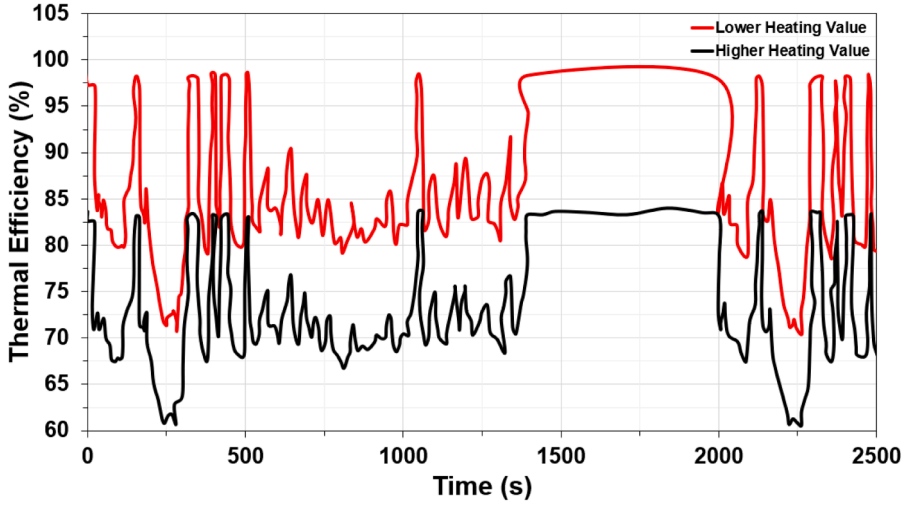

Fig. 9. Thermal efficiency for the fuel cell based on the higher and lower heating values.

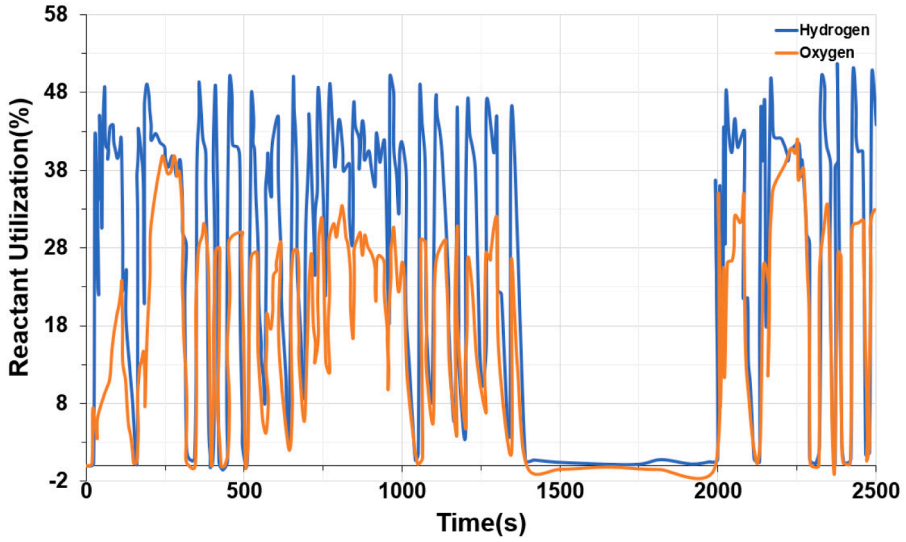

Fig. 10. Percentage reactant utilization within the cell.

4. Organic Rankine Cycle Unit control

In order to operate the ORC system from the transient heat source from the PEM fuel cell in efficient and safe manner, it is essential to adopt robust control approach for the ORC system.

Speed of working fluid pump, expander intake pressure (through the throttling valve), coupled with the exhaust gas mass flow rate were selected as 3 degrees of freedom for the organic Rankine cycle system. The time constants of these 3 degrees of freedom are quite distinct. The set point of the superheat was maintained using a PID controller. The derivative action is based on the error's rate of change, resulting in a controller that reacts quickly to changes in the heat source circumstances. Eqn. 17 captures the control signal for the PID controller.

$$CS(t) = K_p\left[e(t) + \frac{1}{T_i}\int_0^t \{e(t) + track(t)\}dt + \frac{1}{T_d}\frac{de(t)}{dt}\right] \quad (17)$$

The input and output response of the ORC system under active disturbances of the exhaust gas parameters was developed using the dynamic response of the open loop organic Rankine cycle unit. The ziegler – Nichols method was used to find the kp and ki and further validated these values using MATLAB's built-in PID application tool to tune the PID controller using the input and output data from the open loop response. The permitted spectrum of the degree of superheat for the organic Rankine cycle unit is defined by the working fluid decomposition temperature as well as the working fluid condensation temperature. The superheat set point at the expander inlet is set at 2.5 K.

The superheat at the expander inlet is controlled by PID controller. The degree of superheat was chosen as a control variable, whereas pump speed as well as opening/closing of the exhaust gas bypass valve were chosen as process variables. When the exhaust bypass valve is opened, less energy from the exhaust gas may be collected, lowering the system's overall performance. The organic Rankine cycle system's control method is depicted Fig. 6.

5. Result and discussion

5.1. Dynamic response of PEM fuel cell

Fig. 7 captures the overall fuel cell performance for the cell stack. It can be deduced that there is an initial sharp decrease in voltage because

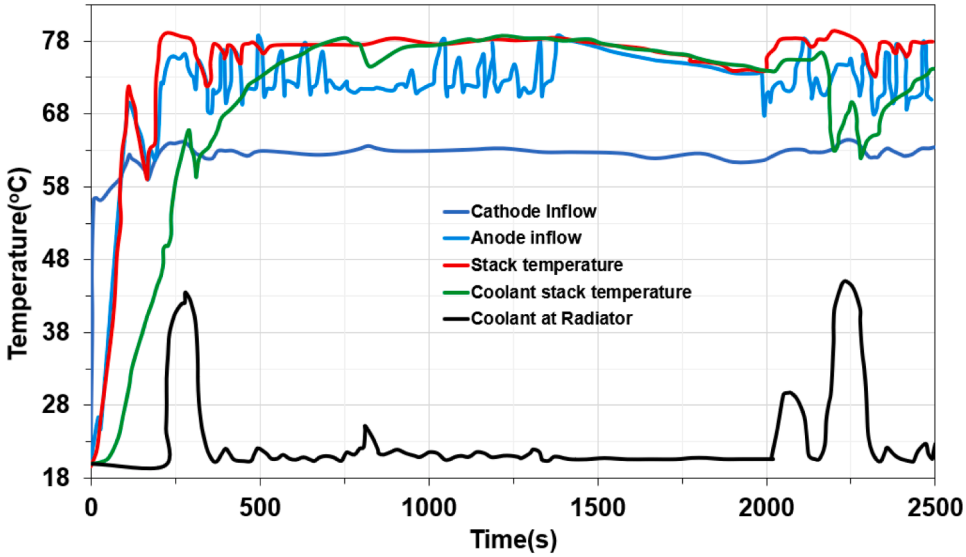

Fig. 11. Temperature various between the various components within the cell.

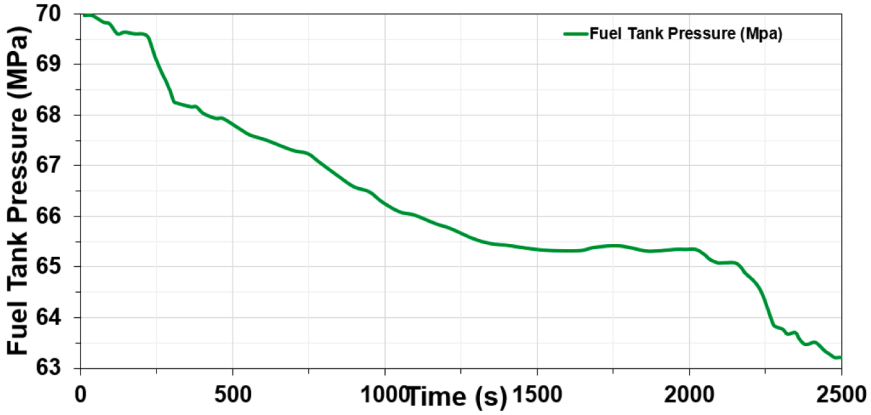

Fig. 12. Fuel tank pressure for the study.

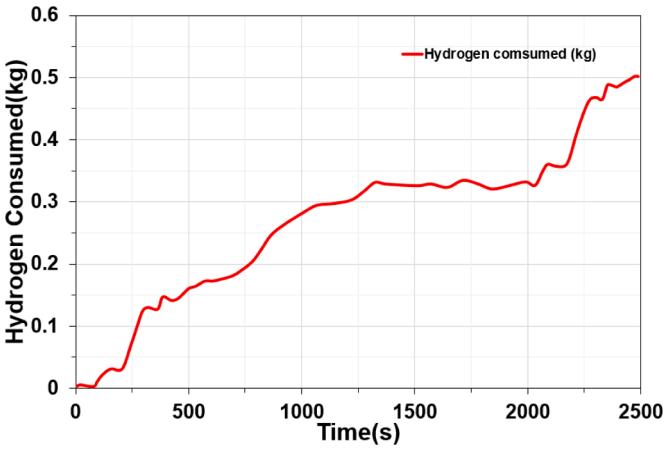

Fig. 13. Hydrogen consumed for 2500 seconds simulation time.

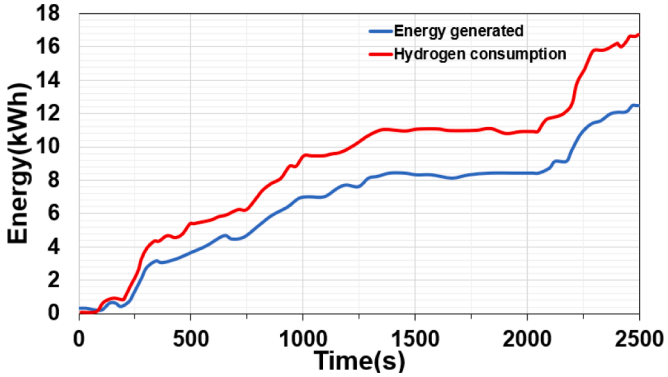

Fig. 14. Rate of energy generated from the fuel cell system in tandem to the hydrogen consumed.

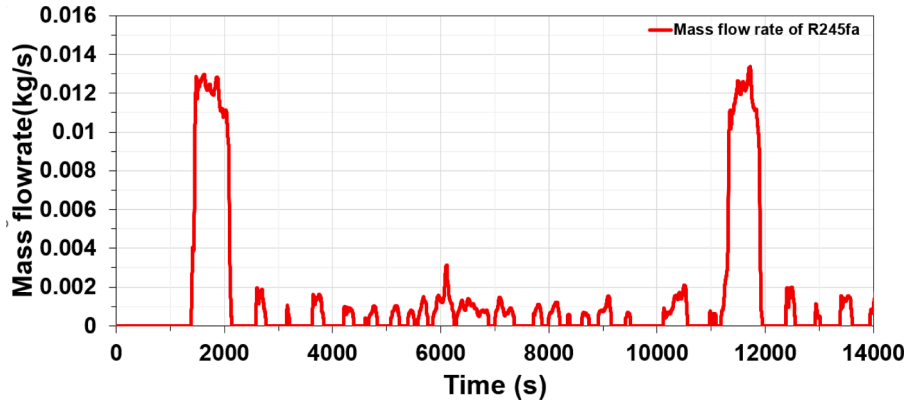

Fig. 15. Mass flowrate of the working fluid.

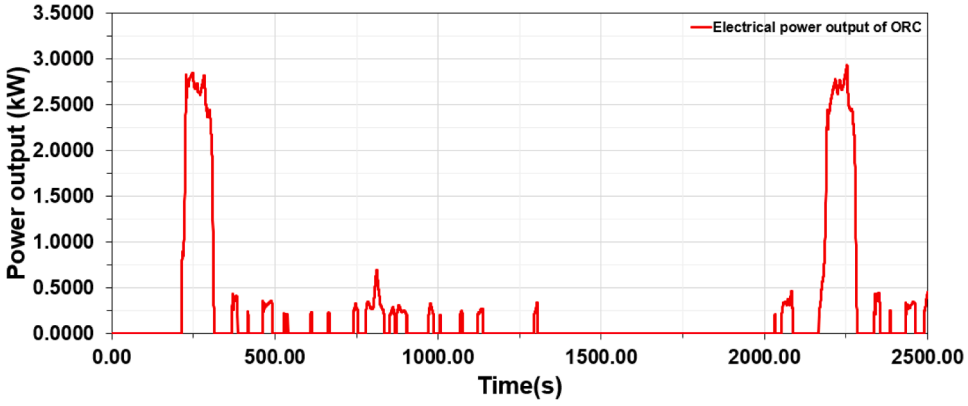

Fig. 16. Electric power generated from the ORC unit.

of activation polarization within the first 5 – 10 seconds of the simulation time. The sudden decrease in voltage becomes gradual after the first 10 seconds due to the effect of ohmic polarization. A reduction in voltage leads to an appreciable increase in current. This phenomenon occurs until the highest attainable current is reached. At the higher current value, there is a further decrease in voltage caused by mass concentration losses. The maximum obtainable power from the fuel cell is also depicted in Fig. 7.

Fig. 8 highlights the power generated from the fuel cell coupled with the power utilised for the air compressor position at the cathodic electrode of the fuel cell as well as that of the coolant pump in other to ensure an efficient mode of operation of the entire system. This therefore explains the justification for the reduction in the total power produced by the entire system as against that produced by the fuel cell.

Captured in Fig. 9 is the thermal performance for the cell coupled with the rate of utilization for the reactant. The thermal performance of the fuel cell basically summarizes fraction of the hydrogen fuel's energy transformed to useful work. Efficiency theoretically is projected to be 83 percent but under experimental conditions, this value goes down to 60 percent because of internal losses. At the highest current density, the efficiency captured is below 50%.

Fig. 10 highlights the amount of hydrogen and oxygen that has gone into reaction within the cell which is described as the reactant utilization. Despite a higher reactant utilization ensure good usage of the reactive substances within the cell, they tend to impact the hydrogen and oxygen concentration negatively thus reducing the generated voltage from the cell. From the developed model, the fuel/hydrogen that does not go into reaction is fed back to the system to curb wastage as well as reduce the cost in running the system. On the other hand, the oxygen that does not go into reaction is released back into the atmosphere. Occasionally, in order to eliminate any form of contaminants, the hydrogen is purged.

The temperature distribution for various sections within the fuel cell unit is presented in Fig. 11. The cell operating temperature was kept constant at 80°C via the cooling system. The hydrogen gas going to the anode was heated by a recirculated flow whiles the oxygen was heated using a compressor. The cooling system was however operated with the aid of controlling the pump flow rate. Fig. 11 equally highlights the coolant temperature once heat is absorbed from the fuel cell as well as when the heat is rejected from the radiator. Figs. 12 and 13 captures the fuel tank pressure as well as the amount of hydrogen consumed during the investigation. Fig. 14 captures the amount of hydrogen consumed and its correlated electrical energy generated.

5.2. *Dynamic performance of the ORC*

The dynamic model results of the ORC system are presented in Figs. 15 and 16. The Fig. 15 shows the variation of the mass flow rate of the working fluid in the ORC system over the 14,000 seconds. The variation in the mass flow rate of R245fa shows a similar trend as the quantity of the waste heat from the PEMFC. At the higher amount of the waste heat from PEMFC, the mass flow rate of the R245fa is higher.

The Fig. 16 shows the power output of the ORC system, and it can be observed that the highest power produced by the ORC system is around 2.8kW at 2250 seconds. The higher the waste heat, the higher the power output of the ORC system was observed. However, at certain intervals where the mass flow rate of the waste heat from the PEMFC is negligible, the power output of the ORC becomes zero too.

In order to ensure the safe operation, PID controller was implement. The controller was able to maintain the ORC system as the optimum

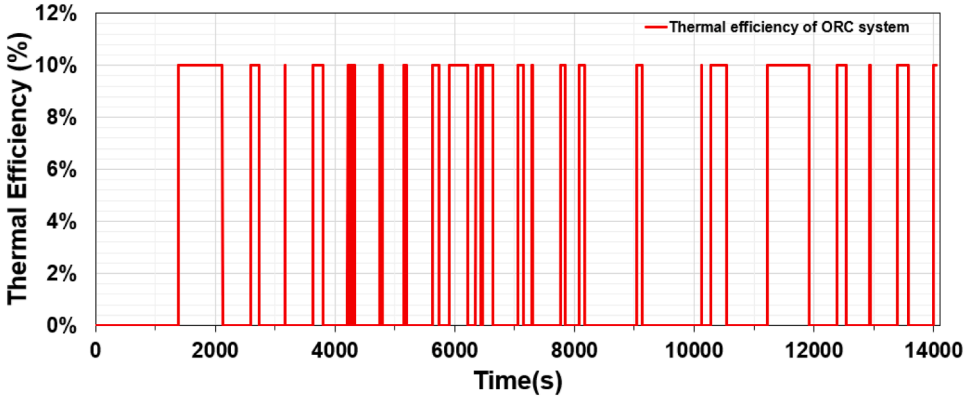

Fig. 17. Thermal Efficiency of the ORC system.

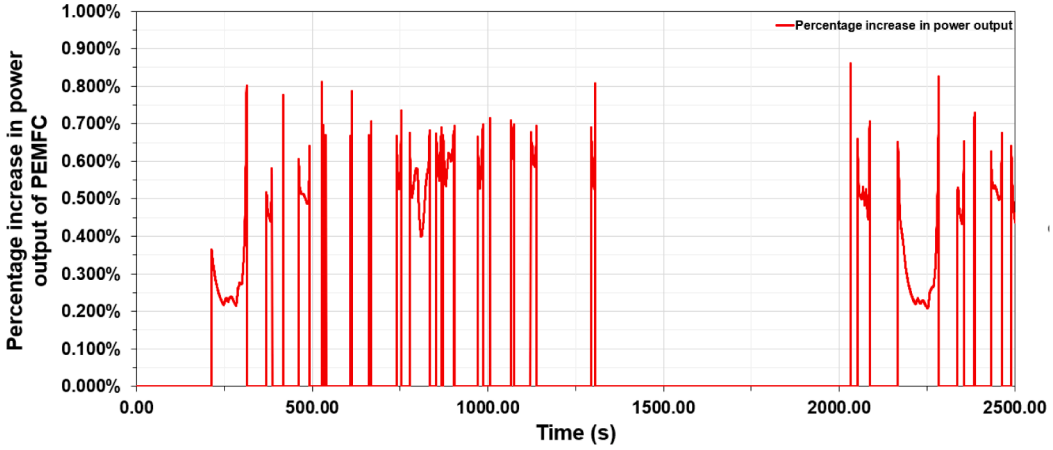

Fig. 18. Percentage increment in power output of the PEMFC for the integrated system.

thermal efficiency of the ORC system, which is 10% in this case (Fig. 17). However, when the ORC system has lower waste heat input, the controller bypasses the working fluid, therefore the power output and thermal efficiency of the ORC system becomes zero.

The dynamic performance of the integrated system is captured in Fig. 18. It can be deduced that there is approximately 0.9% increase in the output power of the fuel cell after 2000 seconds. The margin of increment in terms of power for the combine ORC and PEMFC is subject to the flowrate of the absorbed heat from the heat source. Where there was an appreciable gain in flow rate, there was an appreciable increase in the power being harnessed as well. For scenarios where the flow rate was zero, there percentage increase in power for the PEMFC also presented a sudden drop in terms of the performance of the integrated system.

6. Conclusion

The main goal for the current study was to explore the development of a suitable but ideal proportional integral derivative controller for an ORC unit for the recovery of waste heat from a proton exchange membrane fuel cell unit. The waste heat from the fuel cell was obtained from a cooling unit. Using the object – oriented language (Modelica), a dynamic model was built. Analysis of the dynamic behaviour for the ORC system for open loop process was evaluated in order to obtain data for the input as well as output purposely for tuning the controller. The following conclusions were therefore deduced from the study.

- When the heat source is being operated under transient conditions, variation for the mass flow rate for the working fluid, expander inlet pressure coupled with the degree of superheat tend to have a direct correlation to the exhaust gas mass flowrate.
- Secondly, superheat at the expander inlet can be kept constant via the speed for the working fluid pump as well as partially through the release of exhaust gas into the atmosphere with the aid of an exhaust gas bypass valve.

Due to the present investigation not considering the optimization of the controller, future studies should however explore the development of a predictive model that is ideal for nonlinear scenarios. The present study will serve as basis for information for future studies in the application of proton exchange membrane fuel cells for the marine and automotive industry where heat generated by the cells usually go to waste through their dissipation to the atmosphere. For stationary applications, the present investigation has been able to prove the feasibility in generating more power from the fuel cell in order to improve the overall performance of the integrated system. Similarly, the incorporation of the PID ensured a constant thermal efficiency performance for the ORC system was maintained at 10%. Again, the developed controller is able to quickly respond and monitor effectively the waste heat entering the ORC system and bypass the working fluid by producing zero power output and thermal efficiency for scenarios where the waste heat entering the ORC unit is low.

Declaration of Competing Interest

The authors declare that they have no known competing financial interests or personal relationships that could have appeared to influence the work reported in this paper.

Data availability

Data will be made available on request.

References

[1] Daniel Brough, João Ramos, Bertrand Delpech, Hussam Jouhara, Development and validation of a TRNSYS type to simulate heat pipe heat exchangers in transient applications of waste heat recovery, Int. J. Thermofluids 9 (2021), 100056, https://doi.org/10.1016/j.ijft.2020.100056. ISSN 2666-2027.

[2] José J. Fierro, Ana Escudero-Atehortua, César Nieto-Londoño, Mauricio Giraldo, Hussam Jouhara, Luiz C. Wrobel, Evaluation of waste heat recovery technologies for the cement industry, Int. J. Thermofluids 7–8 (2020), 100040, https://doi.org/10.1016/j.ijft.2020.100040. ISSN 2666-2027.

[3] Youcef Abdellah Ayoub Laouid, Cheikh Kezrane, Yahia Lasbet, Apostolos Pesyridis, Towards improvement of waste heat recovery systems: A multi-objective optimization of different organic Rankine cycle configurations, Int. J. Thermofluids 11 (2021), 100100, https://doi.org/10.1016/j.ijft.2021.100100. ISSN 2666-2027.

[4] M. Venturelli, D Brough, M. Milani, L. Montorsi, Hussam Jouhara, Comprehensive numerical model for the analysis of potential heat recovery solutions in a ceramic industry, Int. J. Thermofluids 10 (2021), 100080, https://doi.org/10.1016/j.ijft.2021.100080. ISSN 2666-2027.

[5] Abdelnasir Omran, Alessandro Lucchesi, David Smith, Abed Alaswad, Amirpiran Amiri, Tabbi Wilberforce, José Ricardo Sodré, A.G. Olabi, Mathematical model of a proton-exchange membrane (PEM) fuel cell, Int. J. Thermofluids 11 (2021), 100110, https://doi.org/10.1016/j.ijft.2021.100110. ISSN 2666-2027.

[6] F.N. Khatib, Tabbi Wilberforce, James Thompson, A.G. Olabi, Experimental and analytical study of open pore cellular foam material on the performance of proton exchange membrane electrolysers, Int. J.Thermofluids 9 (2021), 100068, https://doi.org/10.1016/j.ijft.2021.100068. ISSN 2666-2027.

[7] Y.F. Chang, J. Zhao, S. Shahgaldi, Y.Z. Qin, Y. Yin, X.G. Li, Modelling of mechanical microstructure changes in the catalyst layer of a polymer electrolyte membrane fuel cell, Int. J. Hydrogen Energy (2018), https://doi.org/10.1016/j.ijhydene.2018.10.157. Advance online publication.

[8] Ahmad Baroutaji, Arun Arjunan, Mohamad Ramadan, John Robinson, Abed Alaswad, Mohammad Ali Abdelkareem, Abdul-Ghani Olabi, Advancements and prospects of thermal management and waste heat recovery of PEMFC, Int. J. Thermofluids 9 (2021), 100064, https://doi.org/10.1016/j.ijft.2021.100064. ISSN 2666-2027.

[9] J. Zhao, S. Shahgaldi, X.G. Li, Z.S. Liu, Experimental observations of microstructure changes in the catalyst layers of proton exchange membrane fuel cells under wet-dry cycles, J. Electrochem. Soc. 165 (6) (2018) F3337–F3345, https://doi.org/10.1149/2.0391806jes.

[10] J.J. Baschuk, X.G. Li, Modelling of polymer electrolyte membrane fuel cell stacks based on a hydraulic network approach, Int. J. Energy Res. 28 (8) (2004) 697–724, https://doi.org/10.1002/er.993.

[11] Y.Z. Qin, G.K. Liu, Y.F. Chang, Q. Du, Modeling and design of PEM fuel cell stack based on a flow network method, Appl. Therm. Eng. 144 (2018) 411–423, https://doi.org/10.1016/j.applthermaleng.2018.08.050.

[12] Y.Z. Qin, Q. Du, M.Z. Fan, Y.F. Chang, Y. Yin, Study on the operating pressure effect on the performance of a proton exchange membrane fuel cell power system, Energy Convers. Manage. 142 (2017) 357–365, https://doi.org/10.1016/j.enconman.2017.03.035.

[13] J. Park, X.G. Li, Effect of flow and temperature distribution on the performance of a PEM fuel cell stack, J. Power Sources 162 (1) (2006) 444–459, https://doi.org/10.1016/j.jpowsour.2006.07.030.

[14] G. Karimi, X.G. Li, Analysis and modeling of PEM fuel cell stack performance: Effect of in situ reverse water gas shift reaction and oxygen bleeding, J. Power Sources 159 (2) (2006) 943–950, https://doi.org/10.1016/j.jpowsour.2005.11.104.

[15] K. Nikiforow, P. Koski, J. Ihonen, Discrete ejector control solution design, characterization, and verification in a 5 kW PEMFC system, Int. J. Hydrogen Energy 42 (26) (2017) 16760–16772, https://doi.org/10.1016/j.ijhydene.2017.05.151.

[16] Yin, Y., M. Z. Fan, K. Jiao, Q. Du, and Y. Z. Qin. 2016. Numerical investigation of an ejector for anode recirculation in proton exchange membrane fuel cell system. Energy Convers. Manage.. 126:1106–17. doi:10.1016/j.enconman.2016.09.024.

[17] I.S. Han, S.K. Park, C.B. Chung, Modeling and operation optimization of a proton exchange membrane fuel cell system for maximum efficiency, Energy Convers. Manage. 113 (2016) 52–65, https://doi.org/10.1016/j.enconman.2016.01.045.

[18] M. Alam, K. Kumar, V. Dutta, Dynamic modeling and experimental analysis of waste heat recovery from the proton exchange membrane fuel cell using thermoelectric generator, Therm. Sci. Eng. Prog. 19 (2020), 100627, https://doi.org/10.1016/j.tsep.2020.100627.

[19] J.Y. Lee, J.H. Lee, T.S. Kim, Thermo-economic analysis of using an organic Rankine cycle for heat recovery from both the cell stack and reformer in a PEMFC for power generation, Int. J. Hydrogen Energy 44 (2019) 3876–3890, https://doi.org/10.1016/j.ijhydene.2018.12.071.

[20] Ajarostaghi, S. S. M., and M. A. Delavar. 2018. Waste heat recovery from a 1180 kW proton exchange membrane fuel cell (PEMFC) system by Recuperative organic Rankine cycle (RORC). Energy 157:353–66. doi:10.1016/j.energy.2018.05.132.

[21] Abrar E Elahi, Tahir Mahmud, Mahmodul Alam, Jahangir Hossain, Bapti Niloy Biswas, Exergy analysis of organic Rankine cycle for waste heat recovery using low GWP refrigerants, Int. J. Thermofluids 16 (2022), 100243, https://doi.org/10.1016/j.ijft.2022.100243. ISSN 2666-2027.

[22] A.G. Olabi, Mohammed Al-Murisi, Hussein M. Maghrabie, Bashria AA Yousef, Enas Taha Sayed, Abdul Hai Alami, Mohammad Ali Abdelkareem, Potential applications of thermoelectric generators (TEGs) in various waste heat recovery systems, Int. J. Thermofluids 16 (2022), 100249, https://doi.org/10.1016/j.ijft.2022.100249. ISSN 2666-2027.

[23] Daniel Brough, Hussam Jouhara, The aluminium industry: A review on state-of-the-art technologies, environmental impacts and possibilities for waste heat recovery, Int. J. Thermofluids 1–2 (2020), 100007, https://doi.org/10.1016/j.ijft.2019.100007. ISSN 2666-2027.

[24] T.C. Hung, S.K. Wang, C.H. Kuo, B.S. Pei, K.F. Tsai, A study of organic working fluids on system efficiency of an ORC using low-grade energy sources, Energy 35 (3) (2010) 1403–1411, https://doi.org/10.1016/j.energy.2009.11.025.

[25] E.H. Wang, H.G. Zhang, B.Y. Fan, M.G. Ouyang, Y. Zhao, Q.H. Mu, Study of working fluid selection of organic Rankine cycle (ORC) for engine waste heat recovery, Energy 36 (5) (2011) 3406–3418, https://doi.org/10.1016/j.energy.2011.03.041.

[26] M. Ebrahimi, I. Moradpoor, Combined solid oxide fuel cell, micro-gas turbine and organic Rankine cycle for power generation (SOFC-MGT-ORC), Energy Convers. Manage. 116 (2016) 120–133, https://doi.org/10.1016/j.enconman.2016.02.080.

[27] G.Q. Shu, J. Zhao, H. Tian, H.Q. Wei, X.Y. Liang, G.P. Yu, L.N. Liu, Theoretical analysis of engine waste heat recovery by the combined thermo-generator and organic rankine cycle system, in: SAE 2012 World Congress and Exhibition, 2012, https://doi.org/10.4271/2012-01-0636.

[28] X.D. Wang, L. Zhao, J.L. Wang, W.Z. Zhang, X.Z. Zhao, W. Wu, Performance evaluation of a low-temperature solar Rankine cycle system utilizing R245fa, Sol. Energy 84 (3) (2010) 353–364, https://doi.org/10.1016/j. solener.2009.11.004.

[29] H.W. Chang, C. Duan, X.X. Xu, H.C. Pei, S.M. Shu, Z.K. Tu, Technical performance analysis of a micro-combined cooling, heating and power system based on solar energy and high temperature PEMFC, Int. J. Hydrogen Energy 44 (38) (2019) 21080–21089, https://doi.org/10.1016/j.ijhydene.2018.11.217.

[30] H.W. Chang, Z.M. Wan, Y. Zheng, X. Chen, S.M. Shu, Z.K. Tu, S.H. Chan, Energy analysis of a hybrid PEMFC-solar energy residential micro-CCHP system combined with an organic Rankine cycle and vapor compression cycle, Energy Convers. Manage. 142 (2017) 374–384, https://doi.org/10.1016/j.enconman.2017.03.057.

[31] Colleen Spiegel, Designing and Building Fuel Cells, McGraw Hill, 2007. ISBN-10: 0071489770PublisherIllustrated edition16 July.

[32] Frano Barbir. PEM Fuel Cells, Theory and Practice. Hardcover ISBN: 9780123877109.

[33] Muhammad Imran, Roberto Pili, Muhammad Usman, Fredrik Haglind, Dynamic modeling and control strategies of organic Rankine cycle systems: Methods and challenges, Appl. Energy 276 (2020), 115537, https://doi.org/10.1016/j.apenergy.2020.115537. ISSN 0306-2619.

[34] A Desideri, A Hernandez, S Gusev, M van den Broek, V Lemort, S. Quoilin, Steady-state and dynamic validation of a small-scale waste heat recovery system using the ThermoCycle Modelica library, Energy 115 (2016) 684–696, https://doi.org/10.1016/j.energy.2016.09.004.

[35] F Casella, C. Richter, ExternalMedia: a library for easy re-use of external fluid property code in modelica, in: Proc 6th Int Model Conf, 2008, pp. 157–161.

[36] M. Imran, F. Haglind, Dynamic modelling and development of a reliable control strategy of organic Rankine cycle power systems for waste heat recovery on heavy-duty vehicles, in: Proceedings of ECOS 2019: 32nd International Conference on Efficiency, Cost, Optimization, Simulation and Environmental Impact of Energy Systems, 2019.